

Title

- A selective adenylyl cyclase 1 inhibitor relieves pain without causing tolerance

Running title

- Pain relief through AC1 inhibition

Authors

Gianna Giacoletti¹, Tatum Price¹, Lucas V.B Hoelz², Abdulwhab Shremo Msdi¹, Katerina Vazquez-Falto¹, Tácio V. Amorim Fernandes^{2,3}, Vinícius Santos de Pontes², Hongbing Wang⁴, Nubia Boechat², Adwoa Nornoo¹, Tarsis F. Brust^{1*}

Affiliations

¹ Department of Pharmaceutical Sciences, Lloyd L. Gregory School of Pharmacy, Palm Beach Atlantic University, West Palm Beach, FL, USA 33416.

² Drug Synthesis Laboratory, Drug Technology Institute, Farmanguinhos - FIOCRUZ, Oswaldo Cruz Foundation, Manguinhos, RJ, Brazil 21040900.

³ Instituto Nacional de Metrologia, Qualidade e Tecnologia – INMETRO, Rio de Janeiro, RJ, Brazil 25250020.

⁴ Department of Physiology, Michigan State University, East Lansing, MI, USA 48824.

* Tarsis F. Brust. Tel.: +1 561 803 2757. Fax.: +1 561 803 2703. ORCID:

<https://orcid.org/0000-0003-0912-8273> Email: tarsis_brust@pba.edu

Abstract

Adenylyl cyclases (ACs) catalyze the production of the second messenger cyclic adenosine monophosphate from adenosine triphosphate. Among the ten different AC isoforms, studies with knockout animals indicate that inhibition of AC1 can relieve pain and reduce behaviors linked to opioid dependence. We previously identified ST034307 as a selective inhibitor of AC1. The development of an AC1-selective inhibitor now provides the opportunity to further study the therapeutic potential of inhibiting this protein in pre-clinical animal models of pain and related adverse reactions. In the present study we have shown that ST034307 relieves pain in mouse models of formalin-induced inflammatory pain, acid-induced visceral pain, and acid-depressed nesting. In addition, ST034307 did not cause analgesic tolerance after chronic dosing. We also show that the compound is restricted to the periphery following subcutaneous injections and report the predicted molecular interaction between ST034307 and AC1. Our results indicate that AC1 inhibitors represent a promising new class of analgesic agents that treat pain and appear to produce less adverse effects than currently-used opioids.

Keywords: Adenylyl cyclase, pain, analgesia, AC1, tolerance

51 Introduction

52
53 Adenylyl cyclases (ACs) are the enzymes responsible for catalyzing the conversion of
54 adenosine triphosphate (ATP) into cyclic adenosine monophosphate (cAMP).^{1,2} ACs
55 integrate signaling from a large range of proteins and ions, including G protein-coupled
56 receptors (GPCRs), protein kinases, and calcium, to name a few. There are ten different
57 isoforms of ACs, nine of them are present in the cellular membrane and one is soluble.
58 Each AC isoform has a specific expression pattern, which is related to a specific set of
59 physiological functions.¹ AC isoforms also display a unique set of regulatory properties
60 that result in differences in how the isoforms are modulated by different types of G
61 proteins, protein kinases, and ions.^{1,2}

62 AC1 is part of the group of ACs that are activated by calcium through calmodulin.³
63 Additional regulatory properties of AC1 include inhibition by $G\alpha_{i/o}$ and $G\beta\gamma$ subunits of G
64 proteins and activation by $G\alpha_s$ and the small molecule forskolin.^{1,4} AC1 has also been
65 shown to undergo $G\alpha_{i/o}$ -coupled receptor-mediated superactivation.⁴⁻⁶ The expression
66 pattern of AC1 is consistent with the physiological functions that have been associated
67 with this AC isoform. AC1 transcripts are found in the dorsal root ganglion (DRG), spinal
68 cord, and anterior cingulate cortex (ACC), and a role for this cyclase in pain and
69 nociception has been suggested.⁷⁻⁹ In fact, AC1 knockout (KO) mice display a reduction in
70 typical behaviors that are induced by inflammatory and neuropathic pain, compared to
71 wild-type mice.^{8,10,11} These studies encouraged the pursuit and discovery of novel
72 compounds that can selectively inhibit AC1 activity as potential novel pain-relieving
73 therapeutics.^{4,12,13}

74 AC1 transcripts are also found in the hippocampus, a brain region linked to learning and
75 memory.¹⁴ Notably, AC8, another calcium/calmodulin-activated isoform, is also highly
76 expressed in the hippocampus.^{1,15} Previous studies with single and double AC1/AC8 KO
77 mice have indicated that some functions of AC1 and AC8 related to learning and memory
78 are redundant.¹⁴ Specifically, AC1/AC8 double KO mice display impaired long-term
79 memory in contextual learning and passive avoidance assays, whereas individual KO of
80 each isoform separately results in wild-type-like behaviors.¹⁴ However, each isoform also
81 appears to have specific functions. While less severe deficits are observed in AC1-KO
82 mice compared to the AC1/AC8 double KO, the former still displays reduced long-term
83 potentiation (LTP) in the hippocampus and impairments in certain recognition memory as
84 well as spatial and avoidance learning tasks.^{16,17} Those studies highlight the importance of
85 selectivity for AC1 inhibition versus AC8 for a novel compound to treat pain, but do not
86 exclude the possibility of adverse effects that may result from selective AC1 inhibition in
87 the hippocampus.

88 We have recently reported the discovery of ST034307, a small molecule inhibitor of AC1
89 that is selective for AC1 inhibition versus all other membranous AC isoforms, including
90 AC8.⁴ Our previous study focused on the characterization of ST034307 at the molecular
91 level, showing that the compound is a potent, highly selective, and direct AC1 inhibitor.
92 Moreover, ST034307 was also analgesic in a mouse model of Complete Freund's
93 Adjuvant (CFA)-induced allodynia.⁴ The present study represents a pre-clinical study with
94 ST034307 to determine the potential of this class of compounds as novel analgesic agents.
95 We compared the compound with morphine in mouse models of pain-induced and pain-
96 depressed behaviors and also showed that the compound is restricted to the periphery
97 following subcutaneous injections. Further, we showed that ST034307 does not induce

98 analgesic tolerance or cross-tolerance with morphine. Finally, we expanded our previous
99 mechanistic findings by modeling how the interaction of ST034307 with AC1 happens.

100 101 102 **Materials and Methods**

103 **Experimental design**

104 The main goal of the present study was to determine the potency and efficacy of the AC1
105 selective inhibitor ST034307 in mouse models of pain and innate behavior. Male mice
106 were used as research subjects and sample sizes for the different experiments were
107 determined using power analyses from preliminary experiments following the guidelines
108 of Palm Beach Atlantic University's Institutional Animal Care and Use Committee
109 (IACUC) to attempt to minimize the numbers of animals used. Instances where the
110 number of animals per group vary in an experiment were the result of additional animals
111 being required for proper blinding when a drug dose had to be added. All animals were
112 randomized to treatments and experimenters performing behavioral measurements and
113 injections were blinded to all compound treatments and doses.

114 115 **Materials**

116 ST034307 (6-Chloro-2-(trichloromethyl)-4H-1-benzopyran-4-one) was purchased from
117 Tocris Bioscience and morphine sulphate from Spectrum Laboratory Products. Acetic
118 acid, lactic acid, Tween 80, and formaldehyde were from Sigma-Aldrich. Dimethyl
119 sulfoxide (DMSO) and 0.9% sterile saline were from Fisher Scientific. ST034307 and
120 morphine were prepared in a vehicle consisting of dimethyl sulfoxide (DMSO), Tween 80,
121 and milli-Q water (1:1:8). Specifically, ST034307 was first dissolved in DMSO and
122 sonicated in a 50°C water bath for 15 minutes. Next, Tween 80 was added, the solution
123 was vortexed, and the sonication was repeated. Warm (37°C) milli-Q water was added and
124 the solution was vortexed immediately before injections. Acetic acid, lactic acid, and
125 formalin were diluted in 0.9% sterile saline.

126 127 **Animals**

128 Male C57BL/6J mice were purchased from Charles Rivers Laboratories. AC1-KO mice
129 were created as previously described and propagated using homozygous breeding using
130 the C57BL/6J background.¹⁷ This particular strain is commonly used in studies related to
131 analgesic agents¹⁸⁻²⁰ and provides a way of comparing the activity of ST034307 with other
132 compounds, given that morphine was used as a positive control. Mice were housed in
133 groups (2-5 per cage) in cages covered with filter tops (micro barrier top from Allentown),
134 in a temperature-controlled room under a 12-hour light/dark cycle. Animals had *ad libitum*
135 access to water and food, as well as nesting material made from pulped virgin cotton fiber
136 (nestlets from Lab Supply) for enrichment. Corn cob bedding (1/4") was used for bedding.
137 Mice between 2 and 5 months of age were used for experiments and were dosed
138 subcutaneously with 10 µl/g of ST034307, morphine, or vehicle solutions. After each
139 experiment, mice were humanely euthanized via cervical dislocation under isoflurane
140 anesthesia (open drop method).

141

142 **Study approval**

143 All experimental procedures involving mice adhered to the National Institutes of Health
144 Animal Care guidelines and were approved by Palm Beach Atlantic University's IACUC
145 (West Palm Beach, FL).

146

147 **Formalin-induced paw licking**

148 The formalin-induced paw licking assay was conducted similarly to previously
149 described.²⁰ Briefly, mice were acclimated to clear testing cylinders for 45 minutes. Next,
150 mice were injected subcutaneously with compounds or vehicle solutions and returned to
151 acrylic cylinders for 15 minutes. Mice were then injected into their right hind paw with 25
152 μ l of 5% formalin using a 25 μ l Hamilton syringe and a 30-gauge needle. Mice were
153 immediately returned to the testing cylinders, and paw licking time was recorded in 5-
154 minute intervals for 40 minutes. The experiment was divided into two different phases.
155 The first represents the time spent licking between 0 and 10 minutes, the second represents
156 the time spent licking between 16 and 40 minutes.

157

158 **Acid-induced writhing**

159 For the acid-induced writhing assay, mice were acclimated to clear testing cylinders for 45
160 minutes. Next, mice were injected subcutaneously with compounds or vehicle solutions
161 and returned to acrylic cylinders for 15 minutes. Mice were then injected intraperitoneally
162 with 0.75% acetic acid (10 μ l/g), returned to the testing cylinders, and the number of
163 abdominal constrictions (stretching movements of the body as a whole, including the hind
164 paws) was counted in 5-minute intervals for 30 minutes as previously described.²¹ For the
165 tolerance assay, mice were injected subcutaneously with either 100 mg/kg morphine or 30
166 mg/kg ST034307 (solubility issues prevented the use of higher doses) once a day for four
167 or eight days. At day four or day eight, acid-induced writhing assays were performed.

168

169 **Nesting**

170 The mouse nesting assay was adapted from methods previously described.²² Mice were
171 single housed and acclimated to their new home cage for three days. During the following
172 three days, mice underwent one nesting session (as described below) per day to acclimate
173 them to handling, the experimental procedure, and the testing room. The last acclimation
174 session included a subcutaneous injection (for compound-inhibited nesting) or a
175 subcutaneous injection and an intraperitoneal injection (for acid-depressed nesting) with
176 0.9% saline. On the day after the third acclimation session, mice were injected
177 subcutaneously with compounds or vehicle and returned to their respective home cages for
178 10 minutes. Mice were transferred to a transfer cage (< 1 minute) and nestlets were placed in
179 each of the 6 different zones of the home cage as previously described.²² Mice were either
180 returned to their home cages (compound-inhibited nesting) or injected intraperitoneally
181 (10 μ l/g) with 1% lactic acid (acid-depressed nesting) and returned to their home cages for
182 nesting periods. Nesting was scored as the number of zones cleared over time.

183

184 **Pharmacokinetic studies**

185 The disposition of ST034307 was studied in male C57BL/6J mice following a single
186 subcutaneous injection (10 mg/kg). Mice were humanely euthanized via decapitation
187 under isoflurane anesthesia (open drop method). Subsequently, brain and blood samples
188 were collected in triplicate at 5-, 25-, 45-, 60-, 120- and 240-minutes post-injection. Blood
189 was centrifuged, plasma collected and stored at -80°C. The analyses of the samples were
190 conducted in the Drug Metabolism and Pharmacokinetics Core at Scripps Research. Brain
191 samples were homogenized with water to form a slurry. ST0304307 was extracted from
192 plasma and brain slurry on solid-supported liquid-liquid extraction cartridges
193 (HyperSep™, SLE, 1g/6ml, Thermo Scientific) and the resultant extract was assayed for
194 ST034307 by tandem mass spectroscopy coupled to HPLC (SCIEX 6500). A plot of
195 plasma ST0304307 concentration versus time was constructed and analyzed for non-
196 compartmental pharmacokinetic parameters - half-life, volume of distribution and
197 clearance (Phoenix, Pharsight, Certara Inc.).

198

199 **Molecular Docking**

200 Construction of the AC1 model

201 The AC1 model was constructed through ab-initio and threading methods on I-Tasser
202 server, considering as input the sequences Phe291-Pro478 and Leu859-1058, registered
203 under the UniProtKB ID Q08828.^{23,24} The globular domain regions were identified using
204 both Pfam and UniProtKB feature viewer, being selected for further refining.²⁵ Local
205 sequence alignments with NCBI's BLAST+ were made between the Q08828 and those
206 from Protein Data Bank (PDB) deposited structures to find experimentally solved
207 structures with magnesium ions, ATP, and Gα_s on their respective sites.^{26,27} Thus, using
208 molecular superpositions on VMD 1.9.3, the cofactors and ligands were extracted from the
209 structure registered as 1CJK on PDB, while Gα_s was extracted from the structure
210 registered as 6R3Q, and positioned into the AC1 model.²⁸ MODELLER 9.25-1 was then
211 used to run 100 cycles of structural optimizations with molecular dynamics, simulated
212 annealing, and conjugated gradient.²⁹ The generated structures were ranked by DOPE-
213 Score and the best model was selected. To verify the structural quality of the best AC1
214 model built, the structure was submitted to the SAVES server, where two programs were
215 selected, PROCHECK (Figs. S1, S2, and S3) and VERIFY 3D (Fig. S4), and to the Swiss-
216 PROT server, using QMEANDisCo algorithm (Fig. S5).³⁰⁻³²

217 Preparation of the ST034307 structure

218 ST034307 was constructed and optimized with the HF/6-31G(d) level of theory using the
219 SPARTAN'16 program (Wavefunction, Inc.).

220 Docking using GOLD 2020.3.0 (Genetic Optimization for Ligand Docking)

221 The molecular docking simulation using the GOLD program was carried out using
222 automatic genetic algorithm parameters settings for the population size, selection-
223 pressure, number of islands, number of operations, niche size, and operator weights
224 (migration, mutation, and crossover).³³ The search space was a 40 Å radius sphere from
225 the 66.215, 105.567, and 81.040 (x, y, and z axes, respectively) coordinates. The scoring
226 function used was ChemPLP, which is the default function for the GOLD program. Thus,

227 the pose with the most positive score (the best interaction) was extracted for further
228 analysis.

229 Docking using AutoDock Vina 1.1.2

230 The PDBQT-formatted files for the AC1 model and ST034307 structure were generated
231 using AutoDock Tools (ADT) scripts.³⁴ Using the AutoDock Vina program, the grid size
232 was set to 65.172 Å × 77.050 Å × 73.559 Å for x, y, and z axes, respectively, and the grid
233 center was chosen using 66.215 (x), 105.567 (y), and 81.040 (z) as coordinates. Each
234 docking run used an exhaustiveness setting of 16 and an energy range of 3 kcal/mol.
235 Consequently, the pose with the lowest energy was extracted for interaction analysis.

237 **Data and statistical analyses**

238 All statistical analyses were carried out using GraphPad Prism 9 software (GraphPad
239 Software Inc.). Data normalization and nonlinear regressions were carried out similarly to
240 previously described.¹⁹ For normalizations (representing a rescaling of the Y axis for
241 enhanced clarity), the maximal possible effect was set as 100% (zero for formalin-induced
242 paw licking and acid-induced writhing, and five for acid-depressed nesting) and the
243 response to vehicle's average as 0%. For compound-inhibited nesting, the response from
244 vehicle's average was defined as 100% and zero to 0%. Normalized data was fitted to
245 three-parameter nonlinear regressions with the top constrained to 100% and the bottom to
246 0% (except for the cases where ST034307 did not reach a full response, where no top
247 constrain was set). All statistical analyses were performed using raw experimental data
248 (without normalization). T tests with Welch's correction were used for comparisons
249 between genotypes, one-way ANOVAs for comparisons within groups, and two-way
250 ANOVAs for time-course evaluations. All ANOVAs where F achieved a statistical level
251 of significance ($p < 0.05$) were followed by Dunnett's corrections.

254 **Results**

256 **ST034307 relieves inflammatory pain, but not acute nociception in mice**

257 We have previously shown that intrathecal administration of ST034307 relieves CFA-
258 mediated allodynia in mice.⁴ Here, we used intraplantar formalin injections to the mice's
259 right hind paws and compared the potency of ST034307 with that of morphine (both
260 administered subcutaneously) for diminishing acute nociception and relieving
261 inflammatory pain. The time spent tending to (licking) the injected paw was recorded
262 (Figs. 1a and 1b). As indicated by previous studies using AC1-KO mice,¹¹ only morphine
263 caused a significant reduction in acute nociception, with an ED₅₀ value equal to 5.87
264 mg/kg [95% CI 0.44 to 8.96] (Fig. 1c - sum of measurements recorded between 0 and 10
265 minutes). No significant effect was observed with ST034307. In contrast, both compounds
266 significantly reduced formalin-induced paw licking in the inflammatory pain phase of the
267 model compared to vehicle and had ED₅₀ values equal to 6.88 mg/kg [95% CI 0.85 to
268 14.05] and 1.67 mg/kg [95% CI 0.35 to 2.43] for ST034307 and morphine, respectively
269 (Fig. 1d – sum of measurements recorded between 16 and 40 minutes).

270 Consistent with the results from wild-type mice, AC1-KO mice did not present a reduction
271 of licking during the acute nociception phase of the experiment compared to wild-type
272 mice ($p = 0.2089$ in unpaired t test – Fig. 1e). In addition, while morphine relieved acute
273 nociception in AC1-KO mice ($p < 0.0001$ in one-way ANOVA), no effects were observed

274 with ST034307 (Fig. 1e). In contrast, AC1-KO mice displayed a significant reduction of
275 licking in the inflammatory phase of the model, compared to wild-type mice ($p < 0.001$ in
276 unpaired t test – Fig. 1f). That reduction was similar to the effect 30 mg/kg ST034307 had
277 in wild-type mice (Fig. 1f). No effects were observed from a dose of 30 mg/kg ST034307
278 in AC1-KO mice. Morphine (10 mg/kg) had a small effect in the inflammatory phase, but
279 it was not significantly different from vehicle ($p = 0.087$ in one-way ANOVA – Fig. 1e).

280 **ST034307 relieves visceral pain and does not induce analgesic tolerance in mice**

281 Visceral pain was induced by an intraperitoneal injection of 0.75% acetic acid. The
282 number of abdominal stretches (writhing) the mice performed over a period of 30 minutes
283 was recorded (Figs. 2a and 2b). Both ST034307 and morphine significantly reduced acid-
284 induced writhing in this model with ED₅₀ values equal to 0.92 mg/kg [95% CI 0.15 to
285 4.41] and 0.89 mg/kg [95% CI 0.40 to 1.52], respectively (Fig. 2c). However, ST034307
286 did not reach full efficacy at doses up to 30 mg/kg. Similarly, AC1-KO mice also only
287 showed a partial reduction of acid-induced writhing in this model, compared to wild-type
288 mice ($p < 0.001$ in unpaired t test, Fig. 2d). This response was not enhanced by 10 mg/kg
289 ST034307, but 3 mg/kg morphine caused a significant reduction of acid-induced writhing
290 in AC1-KO mice ($p < 0.01$ in one-way ANOVA – Fig. 2d).

292 Mice treated chronically with morphine display analgesic tolerance. Tolerance is
293 expressed through the gradual loss in efficacy of a compound's dose over time.³⁵ After
294 four days of daily subcutaneous injections with 100 mg/kg morphine, the efficacy of a 3
295 mg/kg dose of morphine decreased by nearly half (Fig. 2e). At day eight, morphine's
296 efficacy was nearly 20% of its initial response (Fig. 2e). In contrast, daily subcutaneous
297 injections with 30 mg/kg ST034307 (highest dose we were able to inject chronically due
298 to solubility) caused no decrease in the analgesic efficacy of a 10 mg/kg ST034307 dose at
299 day four or day eight (Fig. 2e). Notably, no cross-tolerance was developed between the
300 two compounds (Fig. 2f). Mice treated daily with 100 mg/kg morphine were still fully
301 responsive to 10 mg/kg ST034307 at days four and eight; and mice treated daily with 30
302 mg/kg ST034307 were also fully responsive to 3 mg/kg morphine at days four and eight
303 (Fig. 2f).

304 **ST034307 promotes analgesia in the absence of disruptions in the mouse nesting 305 model**

306 Nesting is an innate mouse behavior that can be disrupted by a number of different
307 stimuli.²² Drugs, stress, and pain can all impede normal nesting behavior, making the
308 model appropriate for detecting possible adverse reactions.³⁶ In the experiment, nesting
309 material (nestlets) was placed in six different zones of a mouse's cage. As the mouse
310 makes its nest, it gathers all nestlets in a single zone.²² We measured the numbers of zones
311 cleared over time. ST034307 did not disrupt nesting behaviors at doses up to 30 mg/kg
312 compared to vehicle (Fig. 3a). Morphine, on the other hand, caused a robust reduction of
313 nesting behavior at 3 mg/kg (Fig. 3b – two-way ANOVA, $p < 0.001$ and $p < 0.01$ at 30
314 and 60 minutes, respectively). Morphine's disruption of nesting behavior at the last time-
315 point of the experiment resulted in an ED₅₀ equal to 3.04 mg/kg [95% CI 1.16 to 11.32]
316 (Fig. 3c).

318 As pain can also disrupt nesting behavior, we next tested whether ST034307 could recover
319 nesting in mice that were treated with 1% lactic acid intraperitoneally. Lactic acid
320 treatment caused a profound reduction in nesting behavior (Figs. 3d and 3e). Mice that

321 were treated with 3, 10, or 30 mg/kg ST034307 displayed a significant increase in nesting
322 behavior compared to vehicle-treated animals (Fig. 3d). For morphine, 0.3 and 1 mg/kg
323 caused a significant recovery of nesting behavior during the assay, with no significant
324 effects from 0.1 or 3 mg/kg (Fig. 3e). ST034307's recovery of nesting behavior at the last
325 time-point of the experiment resulted in an ED₅₀ equal to 1.45 mg/kg [95% CI 0.22 to
326 4.93] (Fig. 3f). As the 3 mg/kg dose of morphine depressed mouse nesting, an ED₅₀ value
327 was not calculated for the compound (Fig. 3e). The ED₅₀ value and partial response of
328 ST034307 in this experiment are consistent with what was observed in the acid-induced
329 writhing assay (Fig. 2c).

331 **ST034307 is restricted to the periphery**

332 Given the positive results from the nesting experiments, we decided to determine the
333 concentrations of ST034307 in plasma and brain of mice at different timepoints
334 following a subcutaneous injection with a dose of 10 mg/kg (Fig. 4). A plasma
335 concentration of 0.44 (\pm 0.08) μ M was observed immediately following the injection at 5
336 minutes. A sharp peak was present 60 minutes after the injection at 1.82 (\pm 0.39) μ M and
337 after 90 minutes, the plasma concentration dropped back to levels similar to the levels
338 before the peak (0.33 μ M \pm 0.09). The half-life of ST034307 was determined to be
339 approximately 161 (\pm 88) minutes and the compound was rapidly cleared (CL/F) from the
340 body at a rate of 305.04 (\pm 22.63) ml/min. ST034307 may be highly tissue bound as its
341 volume of distribution (V/F) of 1619 (\pm 790) ml is much greater than the total body water
342 volume (14.5 ml) of a 24 g (average weight) mouse.³⁷ This type of distribution may also
343 indicate extensive red blood cell uptake. To our surprise, none of the timepoints measured
344 resulted in detectable levels of ST034307 in the brains of those mice. These data indicate
345 that the analgesic properties of ST034307 observed are due to its actions in the periphery.

346 **ST034307 interacts with the interface of C1a and C2a domains of AC1**

347 In order to determine the binding interaction of ST034307 with AC1, we constructed a
348 molecular model of AC1. The results of PROCHECK's Ramachandran regions (Fig. S1),
349 main-chain (Fig. S2), and side-chain parameters (Fig. S3), as well as VERIFY 3D (Fig.
350 S4), and QMEANDisCo (Fig. S5) analyses indicated that the AC1 model was structurally
351 valid to further computational studies. Thus, to predict the binding mode of ST034307 to
352 AC1, we carried out molecular docking simulations using two programs, GOLD 2020.3.0
353 and Autodock Vina 1.1.2.^{33,34} Although these programs present differences concerning
354 their search algorithm and scoring function, the best-predicted poses resulting from the
355 different programs showed similar binding modes (RMSD = 2.35Å) into the AC1 model
356 (Fig. 5a). The binding site was located into a cavity adjacent to the ATP binding pocket
357 and between domains C1a and C2a, at the catalytic site interface. The best predicted pose
358 for ST034307 presents a chemPLP score of 49.36 a.u, using the GOLD software, showing
359 a hydrogen bond with the amine group from the side chain of Lys920 (C2a), and steric
360 interactions with Phe306, Leu350, Cys353, Tyr355, Asp417, Val418, Trp419, Val423,
361 Asn427, and Glu430 from C1a and with Lys920 and Ile922 from C2a (Figs. 5b and S6a).
362 Using Autodock Vina, the best-predicted pose for ST034307 presents an interaction
363 energy value of -6.9 kcal/mol, showing only steric interactions with Phe306, Leu350,
364 Cys353, Tyr355, Asp417, Val418, Trp419, Ser420, Val423, Thr224, and Asn427 from
365 C1a and with Lys920 and Ile922 from C2a (Figs. 5c and S6b).

367

368 Discussion and Conclusions

369 Previous studies using AC1-KO mice have indicated that inhibition of AC1 could be a
370 new strategy to treat pain and opioid dependence.^{8,10,11,38,39} Inspired by those studies, we
371 discovered and characterized ST034307.⁴ The compound displayed remarkable selectivity
372 for inhibition of AC1 vs. all other membrane-bound AC isoforms. And while our previous
373 manuscript focused on the molecular characterization of ST034307, we also showed that
374 the compound relieves pain in a mouse model of CFA-induced allodynia.⁴ Here, those
375 findings were expanded in multiple different ways.

376 First, we focused on the activity of the compound in two different models of pain-induced
377 behaviors. In the first, intraplantar injections with formalin to the hind paws of the mice
378 induce a paw licking behavior that is reflective of pain.⁴⁰ The experiment is divided into
379 two distinct phases. The first phase, which includes the first 10 minutes, represents
380 chemical nociception due to the action of formalin on primary afferent nerve fibers.⁴¹
381 ST034307 had no effects on that phase of the experiment (Fig. 1c). This is consistent with
382 our results with AC1-KO mice (Fig. 1e) and with a previous study that showed that AC1-
383 KO mice do not have increased thresholds to thermal, mechanical, or chemical acute
384 nociception compared to wild-type mice.¹¹ Morphine, in contrast, reduced chemical
385 nociception in both wild-type and AC1-KO mice. The formalin-induced paw licking
386 behavior between minutes 16 and 40 is believed to be caused by the development of an
387 inflammatory reaction that induces nerve sensitization.^{36,40,42} As expected, ST034307
388 caused a reduction in licking behavior during that phase. A reduction of formalin-induced
389 paw licking during that phase was also observed in AC1-KO mice compared to wild-type
390 animals. These data are consistent with previous work showing that AC1-KO mice have
391 an increased threshold to inflammatory pain and indicate a possible use of selective AC1
392 inhibitors to treat this type of pain.¹¹

393 Next, we showed that ST034307 decreases the number of abdominal constrictions
394 (writhing) in mice injected intraperitoneally with acetic acid. Intraperitoneal injections
395 with irritant agents cause peritovisceral pain and previous studies suggest that all
396 analgesics can reduce abdominal cramps in this model.^{36,43} In contrast to morphine,
397 ST034307 did not result in the maximal possible effect in this experiment, an outcome that
398 was mimicked by AC1-KO mice. This partial response allowed us to further confirm that
399 the effect of ST034307 in this model was through AC1 inhibition, as morphine, but not
400 ST034307, further reduced the number of acid-induced abdominal constrictions in AC1-
401 KO mice (Fig. 2d).

402 The use of analgesic agents often requires chronic dosing, which may last days, months, or
403 even years depending on the patient's pain condition. Unfortunately, chronic analgesic
404 dosing may lead to analgesic tolerance.⁴⁴ Opioid tolerance is well documented in humans
405 and rodents, and results in a loss of analgesic efficacy over time.^{19,35,44} At the molecular
406 level, it has been proposed that opioid tolerance is caused by agonist-induced recruitment
407 of β arrestins to the mu opioid receptor (MOR). β arrestins induce receptor internalization
408 (removal from the membrane) and, therefore, reduce the pool of available receptors for
409 opioid action.³⁵ As ST034307 acts as an inhibitor of AC1, the mechanisms commonly
410 linked to tolerance (receptor downregulation) should not be present. Consistently, we did
411 not observe any tolerance to a high daily dose of ST034307 for up to eight days in the

412 mouse acid-induced writhing assay. This is in contrast to morphine, which displayed a
413 marked reduction of analgesic efficacy, consistent with analgesic tolerance. As the two
414 compounds act through different mechanisms (though the MOR inhibits AC1),⁴ there was
415 no observable development of cross-tolerance.

416 Paw licking and abdominal constrictions are examples of pain-stimulated behaviors.
417 While useful in pain studies, a reduction of these behaviors may not necessarily indicate
418 pain relief. Compounds that induce paralysis, sedation, or stimulate a competing behavior,
419 for instance, can still cause a marked reduction of behavior in those experiments, but are
420 not necessarily relieving pain.^{22,36} Therefore, we have employed the pain-depressed
421 behavior of nesting as another method to determine the analgesic efficacy of ST034307.
422 Different types of stimuli (such as pain, stress, and sedation) can cause disruptions of
423 mouse innate behaviors. Therefore, in order for a compound to display pain relief in this
424 model, it may not present disruptive properties, as if it does, nesting behavior will be
425 further reduced (see the 3 mg/kg dose of morphine in Figs. 3c and 3e).²² ST034307 did not
426 disrupt nesting behavior at doses up to 30 mg/kg, indicating good tolerability in this
427 model. Furthermore, all doses that were effective at relieving pain in the previous models,
428 also significantly recovered nesting behavior that was reduced by an intraperitoneal
429 injection of lactic acid (Fig. 3d). According to Negus (2019), the combination of the
430 results from our nesting experiments and our pain-stimulated behavior experiments makes
431 ST034307 (and possibly other AC1-selective inhibitors) a “high-priority” analgesic
432 compound for “further testing”.³⁶

433 While the nesting experiments provide a measure of safety, studies describing the full
434 spectrum of possible adverse reactions that result from AC1 inhibition are still needed
435 (and are underway). The high expression levels of AC1 in the hippocampus suggests that
436 the initial focus of these studies should be on learning and memory. ST034307 is selective
437 for AC1 vs. AC8. Nevertheless, AC1-KO mice still display impaired performance in
438 certain learning and memory tasks.^{4,16,17} The use of a pharmacological agent will allow us
439 to determine if those effects are a result of developmental issues (as AC1 expression is
440 important for synaptic plasticity and development)^{45,46} or if there is an acute dose-
441 dependent effect. If ST034307 is to be used for those experiments, intrathecal or
442 intracerebroventricular injections will be required to ensure that the compound reaches the
443 brain. The development of chronic adverse effects, other than analgesic tolerance, should
444 also be investigated. It is not expected that AC1 inhibitors will be rewarding, but the
445 current state of the opioid crisis indicates that this should be tested experimentally, and the
446 effects of AC1 inhibitors on the release of dopamine in the nucleus accumbens should also
447 be assessed.

448 It is noteworthy that the current experiments were performed with subcutaneous
449 injections, instead of the intrathecal injections from Brust et al., 2017.⁴ This allowed us to
450 determine the disposition of the compound in plasma and brain. The plasma concentration
451 of 10 mg/kg ST034307 peaked at 60 minutes after injection. Notably, we were unable to
452 detect ST034307 in the brain. Nevertheless, the disposition of this compound in plasma
453 indicates a wide distribution in the body and rapid clearance resulting in relatively low
454 concentrations compared to the administered dose. These concentrations persist for at least
455 four hours to account for the effects that are seen in these experiments. These data suggest
456 that the effects observed in the present studies are due to the actions of the compound in
457 the periphery. It has recently been reported that the analgesic effects related to a reduction
458 of AC1 activity is associated with the expression of the enzyme in the DRG and spinal

459 cord.⁹ As the DRG is located in the periphery, it is likely that this is the site responsible
460 for the analgesic properties of ST034307. The fact that ST034307 is not reaching the brain
461 also precludes the compound's activity in the hippocampus and makes it unlikely that this
462 particular compound, when administered subcutaneously, would cause adverse effects
463 related to learning and memory.

464 In the last set of data presented in the manuscript, the interaction between ST034307 and
465 AC1 was mapped using molecular docking. Those results, achieved using of two different
466 programs, suggest that ST034307 interacts at a site located between the ATP and forskolin
467 binding sites. This binding site is located at the interface of the C1a and C2a domains and
468 is indicative of a non-competitive or uncompetitive mechanism. The action of ST034307
469 is proposed to cause a disruption of the structure of AC1's catalytic domain and,
470 consequently, enzymatic inhibition. As our modeling showed that ST034307 does not bind
471 to the ATP binding site, it is consistent with our previous findings that indicate that the
472 compound is not a P-site inhibitor.^{1,4}

473 As encouraging as the data presented in the manuscript appears, other compounds that
474 looked promising in pre-clinical models of pain have failed to translate to clinic.³⁶ While
475 the nesting experiments account for some adverse effects and competing behaviors that
476 may generate false positives, additional studies on ST034307 and the class of AC1
477 inhibitors are still needed. Particular attention should be devoted to possible impairments
478 on learning and memory as well as other models of pain that reflect pain states that are
479 different from the ones already examined. Experiments with AC1 inhibitors that can reach
480 the brain are also desired. Nevertheless, the present work clearly demonstrates a
481 correlation between selective inhibition of AC1 and behaviors that are consistent with
482 analgesia in mice. More work is still needed to establish this class of compounds as novel
483 pain therapeutics; however, the present study represents an important step that may signal
484 that selective AC1 inhibitors should be prioritized for further testing and advancement for
485 the treatment of pain.

486 487 488 **Supplementary Materials**

489 Fig. S1. Ramachandran plot statistics analysis of the adenylyl cyclase 1 model.

490 Fig. S2. Main-chain stereochemical parameters statistical analysis of the adenylyl cyclase
491 1 model.

492 Fig. S3. Side-chain stereochemical parameters statistical analysis of the adenylyl cyclase 1
493 model.

494 Fig. S4. Three-dimensional profile analysis of the adenylyl cyclase 1 model.

495 Fig. S5. QMEANDisCo analysis of the adenylyl cyclase 1 model.

496 Fig. S6. 2D representation of the ST034307 poses.

497
498
499 **Data and materials availability:** All data required to evaluate the conclusions in the paper are
500 present in the manuscript or references. Materials will be made available upon request.

501 502 **Acknowledgements**

503 Funding: This work is supported by the American Association of Colleges of Pharmacy's
504 New Investigator Award (T.F.B.), the Lloyd L. Gregory School of Pharmacy's
505

IntegraConnect grant (T.F.B and A.N.), and Palm Beach Atlantic University's Quality Initiative grant (T.F.B.), Fundação Carlos Chagas Filho de Amparo à Pesquisa do Estado do Rio de Janeiro (FAPERJ) (N.B.), Conselho Nacional de Desenvolvimento Científico e Tecnológico (CNPq), Fundação de Apoio à Fiocruz (FIOTEC) (N.B.), Coordenação de Aperfeiçoamento de Pessoal de Nível Superior (CAPES) – Finance Code 001 (N.B.), and Programa Nacional de Apoio ao Desenvolvimento da Metrologia, Qualidade e Tecnologia (PRONAMETRO) from Instituto Nacional de Metrologia, Qualidade e Tecnologia (INMETRO) (T.V.A.F.).

Author Contributions: Conceptualization: T.F.B. Experimental design: T.F.B., G.G., A.N., L.V.B.H. Performed experiments: T.F.B., G.G., T.P., L.V.B.H., A.S.M., T.V.A.F., V.S.P. Data analyses: T.F.B., L.V.B.H., A.N. Provided needed equipment or materials: N.B., H.W. Writing: T.F.B. wrote the first draft of the manuscript and all authors contributed, reviewed, and edited.

Competing Financial Interests statement: The authors have no competing interests.

References

- 1 Dessauer, C. W. *et al.* International Union of Basic and Clinical Pharmacology. CI. Structures and Small Molecule Modulators of Mammalian Adenylyl Cyclases. *Pharmacol Rev* **69**, 93-139, doi:10.1124/pr.116.013078 (2017).
- 2 Cooper, D. & Crossthwaite, A. Higher-order organization and regulation of adenylyl cyclases. *Trends Pharmacol Sci* **27**, 426-431, doi:10.1016/j.tips.2006.06.002 (2006).
- 3 Masada, N., Schaks, S., Jackson, S. E., Sinz, A. & Cooper, D. M. Distinct mechanisms of calmodulin binding and regulation of adenylyl cyclases 1 and 8. *Biochemistry* **51**, 7917-7929, doi:10.1021/bi300646y (2012).
- 4 Brust, T. F. *et al.* Identification of a selective small-molecule inhibitor of type 1 adenylyl cyclase activity with analgesic properties. *Sci Signal* **10**, doi:10.1126/scisignal.aah5381 (2017).
- 5 Brust, T. F., Conley, J. M. & Watts, V. J. Galphai/o-coupled receptor-mediated sensitization of adenylyl cyclase: 40 years later. *Eur J Pharmacol* **763**, 223-232, doi:10.1016/j.ejphar.2015.05.014 (2015).
- 6 Cumbay, M. & Watts, V. Heterologous sensitization of recombinant adenylate cyclases by activation of D(2) dopamine receptors. *J Pharmacol Exp Ther.* **297**, 297(293) (2001).
- 7 Wei, F. *et al.* Calcium calmodulin-stimulated adenylyl cyclases contribute to activation of extracellular signal-regulated kinase in spinal dorsal horn neurons in adult rats and mice. *J Neurosci* **26**, 851-861, doi:10.1523/JNEUROSCI.3292-05.2006 (2006).
- 8 Xu, H. *et al.* Presynaptic and postsynaptic amplifications of neuropathic pain in the anterior cingulate cortex. *J Neurosci* **28**, 7445-7453, doi:10.1523/JNEUROSCI.1812-08.2008 (2008).
- 9 Johnson, K., Doucette, A., Edwards, A., Watts, V. J. & Klein, A. H. Reduced activity of Adenylyl Cyclase 1 Attenuates Morphine Induced Hyperalgesia and Inflammatory Pain in Mice. *bioRxiv*, 2020.2012.2002.408419, doi:10.1101/2020.12.02.408419 (2020).
- 10 Vadakkan, K. I. *et al.* Genetic reduction of chronic muscle pain in mice lacking calcium/calmodulin-stimulated adenylyl cyclases. *Mol Pain* **2**, 7, doi:10.1186/1744-8069-2-7 (2006).

- 555 11 Wei, F. *et al.* Genetic elimination of behavioral sensitization in mice lacking calmodulin-
556 stimulated adenylyl cyclases. *Neuron* **36**, 713-726 (2002).
- 557 12 Brand, C. S., Hocker, H. J., Gorfe, A. A., Cavasotto, C. N. & Dessauer, C. W. Isoform
558 selectivity of adenylyl cyclase inhibitors: characterization of known and novel
559 compounds. *J Pharmacol Exp Ther* **347**, 265-275, doi:10.1124/jpet.113.208157 (2013).
- 560 13 Kaur, J. *et al.* Optimization of a 1,3,4-oxadiazole series for inhibition of
561 Ca(2+)/calmodulin-stimulated activity of adenylyl cyclases 1 and 8 for the treatment of
562 chronic pain. *Eur J Med Chem* **162**, 568-585, doi:10.1016/j.ejmech.2018.11.036 (2018).
- 563 14 Wong, S. T. *et al.* Calcium-stimulated adenylyl cyclase activity is critical for
564 hippocampus-dependent long-term memory and late phase LTP. *Neuron* **23**, 787-798
565 (1999).
- 566 15 Wang, H. *et al.* Type 8 adenylyl cyclase is targeted to excitatory synapses and required for
567 mossy fiber long-term potentiation. *J Neurosci* **23**, 9710-9718 (2003).
- 568 16 Shan, Q., Chan, G. C. & Storm, D. R. Type 1 adenylyl cyclase is essential for maintenance
569 of remote contextual fear memory. *J Neurosci* **28**, 12864-12867,
570 doi:10.1523/JNEUROSCI.2413-08.2008 (2008).
- 571 17 Zheng, F. *et al.* Voluntary running depreciates the requirement of Ca²⁺-stimulated cAMP
572 signaling in synaptic potentiation and memory formation. *Learn Mem* **23**, 442-449,
573 doi:10.1101/lm.040642.115 (2016).
- 574 18 Brust, T. F. *et al.* Biased agonists of the kappa opioid receptor suppress pain and itch
575 without causing sedation or dysphoria. *Sci Signal* **9**, ra117, doi:10.1126/scisignal.aai8441
576 (2016).
- 577 19 Grim, T. W. *et al.* A G protein signaling-biased agonist at the mu-opioid receptor reverses
578 morphine tolerance while preventing morphine withdrawal. *Neuropsychopharmacology*
579 **45**, 416-425, doi:10.1038/s41386-019-0491-8 (2020).
- 580 20 Pantouli, F. *et al.* Comparison of morphine, oxycodone and the biased MOR agonist SR-
581 17018 for tolerance and efficacy in mouse models of pain. *Neuropharmacology* **185**,
582 108439, doi:10.1016/j.neuropharm.2020.108439 (2021).
- 583 21 Tarselli, M. A. *et al.* Synthesis of conolidine, a potent non-opioid analgesic for tonic and
584 persistent pain. *Nat Chem* **3**, 449-453, doi:10.1038/nchem.1050 (2011).
- 585 22 Negus, S. S. *et al.* Effects of ketoprofen, morphine, and kappa opioids on pain-related
586 depression of nesting in mice. *Pain* **156**, 1153-1160,
587 doi:10.1097/j.pain.000000000000171 (2015).
- 588 23 Yang, J. & Zhang, Y. I-TASSER server: new development for protein structure and
589 function predictions. *Nucleic Acids Res* **43**, W174-181, doi:10.1093/nar/gkv342 (2015).
- 590 24 UniProt, C. UniProt: the universal protein knowledgebase in 2021. *Nucleic Acids Res* **49**,
591 D480-D489, doi:10.1093/nar/gkaa1100 (2021).
- 592 25 Mistry, J. *et al.* Pfam: The protein families database in 2021. *Nucleic Acids Res* **49**, D412-
593 D419, doi:10.1093/nar/gkaa913 (2021).
- 594 26 Altschul, S. F., Gish, W., Miller, W., Myers, E. W. & Lipman, D. J. Basic local alignment
595 search tool. *J Mol Biol* **215**, 403-410, doi:10.1016/S0022-2836(05)80360-2 (1990).
- 596 27 Berman, H. M. *et al.* The Protein Data Bank. *Acta Crystallogr D Biol Crystallogr* **58**, 899-
597 907, doi:10.1107/s0907444902003451 (2002).
- 598 28 Humphrey, W., Dalke, A. & Schulten, K. VMD: visual molecular dynamics. *J Mol Graph*
599 **14**, 33-38, 27-38, doi:10.1016/0263-7855(96)00018-5 (1996).
- 500 29 Sali, A. & Blundell, T. L. Comparative protein modelling by satisfaction of spatial
501 restraints. *J Mol Biol* **234**, 779-815, doi:10.1006/jmbi.1993.1626 (1993).
- 502 30 Colovos, C. & Yeates, T. O. Verification of protein structures: patterns of nonbonded
503 atomic interactions. *Protein Sci* **2**, 1511-1519, doi:10.1002/pro.5560020916 (1993).

- 504 31 Studer, G. *et al.* QMEANDisCo-distance constraints applied on model quality estimation.
505 *Bioinformatics* **36**, 1765-1771, doi:10.1093/bioinformatics/btz828 (2020).
- 506 32 Laskowski, R. A., MacArthur, M. W., Moss, D. S. & Thornton, J. M. PROCHECK: a
507 program to check the stereochemical quality of protein structures. *Journal of Applied*
508 *Crystallography* **26**, 283-291, doi:doi:10.1107/S0021889892009944 (1993).
- 509 33 Jones, G., Willett, P., Glen, R. C., Leach, A. R. & Taylor, R. Development and validation
510 of a genetic algorithm for flexible docking. *J Mol Biol* **267**, 727-748,
511 doi:10.1006/jmbi.1996.0897 (1997).
- 512 34 Trott, O. & Olson, A. J. AutoDock Vina: improving the speed and accuracy of docking
513 with a new scoring function, efficient optimization, and multithreading. *J Comput Chem*
514 **31**, 455-461, doi:10.1002/jcc.21334 (2010).
- 515 35 Raehal, K. M., Schmid, C. L., Groer, C. E. & Bohn, L. M. Functional selectivity at the
516 mu-opioid receptor: implications for understanding opioid analgesia and tolerance.
517 *Pharmacol Rev* **63**, 1001-1019, doi:10.1124/pr.111.004598 (2011).
- 518 36 Negus, S. S. Core Outcome Measures in Preclinical Assessment of Candidate Analgesics.
519 *Pharmacol Rev* **71**, 225-266, doi:10.1124/pr.118.017210 (2019).
- 520 37 Davies, B. & Morris, T. Physiological parameters in laboratory animals and humans.
521 *Pharm Res* **10**, 1093-1095, doi:10.1023/a:1018943613122 (1993).
- 522 38 Zachariou, V. *et al.* Distinct roles of adenylyl cyclases 1 and 8 in opiate dependence:
523 behavioral, electrophysiological, and molecular studies. *Biol Psychiatry* **63**, 1013-1021,
524 doi:10.1016/j.biopsych.2007.11.021 (2008).
- 525 39 Luo, J., Phan, T. X., Yang, Y., Garelick, M. G. & Storm, D. R. Increases in cAMP,
526 MAPK activity, and CREB phosphorylation during REM sleep: implications for REM
527 sleep and memory consolidation. *J Neurosci* **33**, 6460-6468,
528 doi:10.1523/JNEUROSCI.5018-12.2013 (2013).
- 529 40 Tjolsen, A., Berge, O. G., Hunskaar, S., Rosland, J. H. & Hole, K. The formalin test: an
530 evaluation of the method. *Pain* **51**, 5-17, doi:10.1016/0304-3959(92)90003-T (1992).
- 531 41 McNamara, C. R. *et al.* TRPA1 mediates formalin-induced pain. *Proc Natl Acad Sci U S*
532 *A* **104**, 13525-13530, doi:10.1073/pnas.0705924104 (2007).
- 533 42 Woolf, C. J. Evidence for a central component of post-injury pain hypersensitivity. *Nature*
534 **306**, 686-688, doi:10.1038/306686a0 (1983).
- 535 43 Collier, H. O., Dinneen, L. C., Johnson, C. A. & Schneider, C. The abdominal constriction
536 response and its suppression by analgesic drugs in the mouse. *Br J Pharmacol Chemother*
537 **32**, 295-310 (1968).
- 538 44 Stein, C. Opioid Receptors. *Annu Rev Med* **67**, 433-451, doi:10.1146/annurev-med-
539 062613-093100 (2016).
- 540 45 Haupt, C., Langhoff, J. & Huber, A. B. Adenylate Cyclase 1 modulates peripheral nerve
541 branching patterns. *Mol Cell Neurosci* **45**, 439-448, doi:10.1016/j.mcn.2010.08.003
542 (2010).
- 543 46 Wang, H., Liu, H., Storm, D. R. & Zhang, Z. W. Adenylate cyclase 1 promotes
544 strengthening and experience-dependent plasticity of whisker relay synapses in the
545 thalamus. *J Physiol* **589**, 5649-5662, doi:10.1113/jphysiol.2011.213702 (2011).
- 546 47 Pettersen, E. F. *et al.* UCSF Chimera--a visualization system for exploratory research and
547 analysis. *J Comput Chem* **25**, 1605-1612, doi:10.1002/jcc.20084 (2004).
- 548
549
550
551
552
553

Figure Legends

Fig. 1. ST034307 relieves inflammatory pain in mice. (a) Different doses of ST034307 reduce paw licking behavior caused by an intraplantar injection with 5% formalin. (b) Different doses of morphine reduce paw licking behavior caused by an intraplantar injection with 5% formalin. (c) Dose-response curves of the sum of time spent licking the paw during the first 10 minutes of the graphs in A and B. Vehicle's response was set as 0% and the maximal possible effect (0) to 100%. (d) Dose-response curves of the sum of time spent licking the paw during the period in between minute 16 and minute 40 of the graphs in A and B. Vehicle's response was set as 0% and the maximal possible effect (0) to 100%. (e) Reduction of time spent licking the injected paw in wild-type (WT) and in AC1-KO mice treated with vehicle (V), 30 mg/kg ST034307 (S), or 10 mg/kg morphine (M) during the first 10 minutes of the experiment. (f) Reduction of time spent licking the injected paw in wild-type (WT) and in AC1-KO mice treated with vehicle (V), 30 mg/kg ST034307 (S), or 10 mg/kg morphine (M) during the first 10 minutes of the experiment. For E and F vehicle's response in wild-type mice was set to 0% and zero to 100%. Data in all graphs represent the average \pm S.E.M., N = 6-8. **** $p < 0.0001$ in one-way ANOVA with Dunnett's test.

Fig. 2. ST034307 relieves visceral pain in mice. (a) Different doses of ST034307 reduce the number of abdominal constrictions caused by an intraperitoneal injection with 0.75% acetic acid; N = 8-10. (b) Different doses of morphine reduce the number of abdominal constrictions caused by an intraperitoneal injection with 0.75% acetic acid; N=8-10. (c) Dose-response curves of the total number of abdominal constrictions from the graphs in A and B. Vehicle's response was set as 0% and the maximal possible effect (0) to 100%. (d) Reduction of the total number of abdominal constrictions in wild-type (WT) and in AC1-KO mice treated with vehicle (V), 30 mg/kg ST034307 (S), or 10 mg/kg morphine (M). Vehicle's response in wild-type mice was set as 0% and zero to 100%; N = 5. (e) Mice were injected daily with 30 mg/kg ST034307 or 100 mg/kg morphine and on day four or eight acid-induced writhing assays were performed. Mice that chronically received morphine displayed a decrease in efficacy of 3 mg/kg morphine on days four or eight, compared to a group of mice that received vehicle plus 3 mg/kg morphine on day zero. Mice that chronically received ST034307 did not display any changes in efficacy of 10 mg/kg ST034307; N = 5. (f) Mice were injected daily with 30 mg/kg ST034307 or 100 mg/kg morphine and on day four or eight acid-induced writhing assays were performed. Mice that chronically received morphine did not display any changes in efficacy with 10 mg/kg ST034307. Mice that chronically received ST034307 did not display any changes in efficacy with 3 mg/kg morphine; N = 5. Data in all graphs represent the average \pm S.E.M. * $p < 0.05$, ** $p < 0.01$, *** $p < 0.001$ in one-way ANOVA with Dunnett's test.

Fig. 3. ST034307 rescues acid-depressed mouse nesting behavior. (a) ST034307 did not reduce mouse nesting behavior at doses up to 30 mg/kg. (b) At a dose of 3 mg/kg, morphine significantly reduced mouse nesting behavior at 30 and 60 minutes after nesting measurements were started. (c) Dose-response curves of the last experimental timepoints the graphs in A and B. Vehicle's response was set as 100% and the maximal possible effect (0) to 0%. (d) and (e) 3 mg/kg, 10 mg/kg, and 30 mg/kg ST034307 and 1 mg/kg morphine significantly rescued mouse

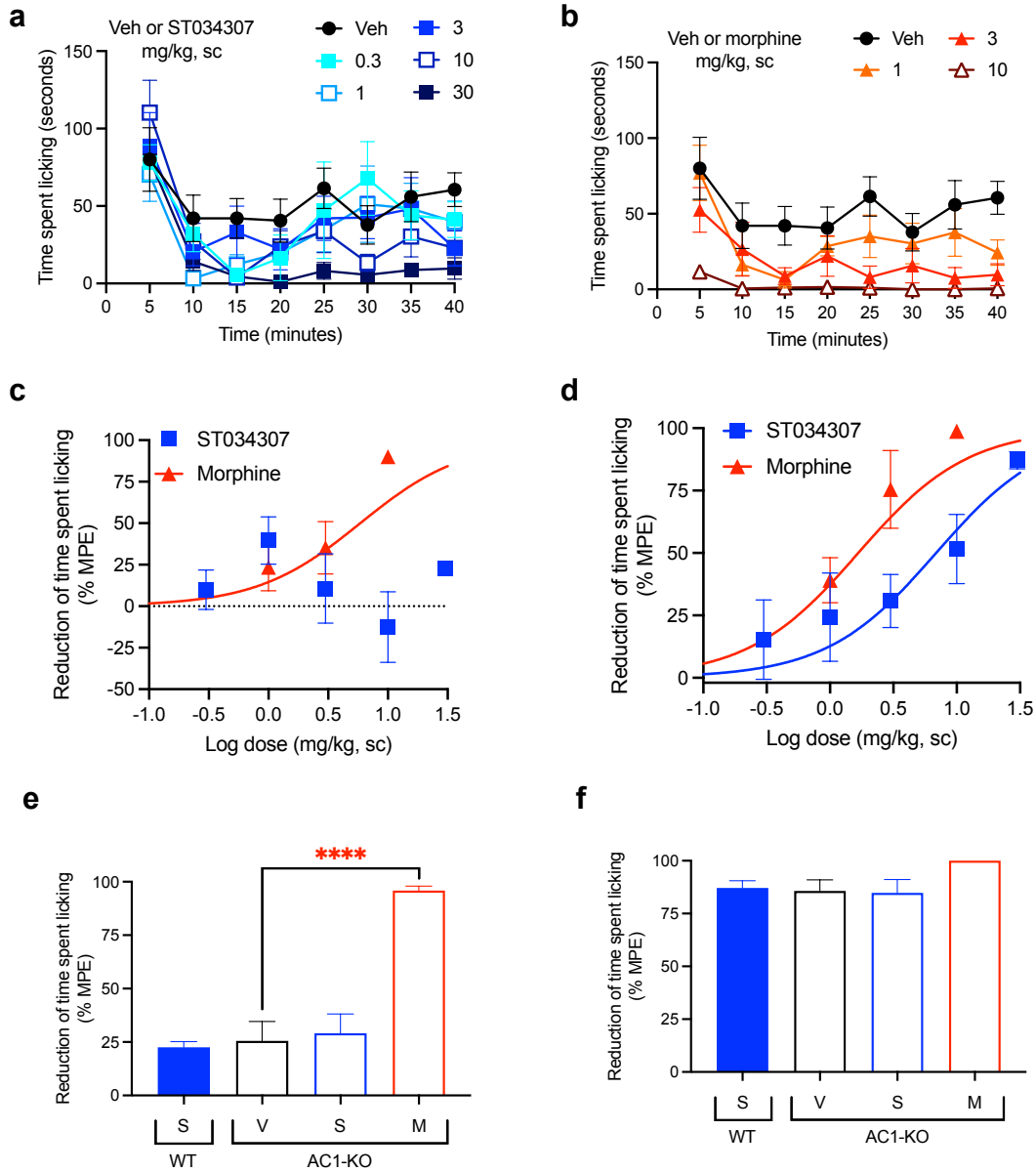
704 nesting behavior that was reduced by an intraperitoneal injection of 1% lactic acid.
705 (f) Dose-response curves of the last experimental timepoints from the graphs in D
706 and E. Vehicle's response was set as 0% and the maximal possible effect (5) to
707 100%. Data in all graphs represent the average \pm S.E.M., N = 6-8. * p < 0.05, ** p <
708 0.01, *** p < 0.001 in two-way ANOVA with Dunnett's test.
709

710 **Fig. 4. Plasma ST0304307 concentration versus time profile after a single**
711 **subcutaneous injection in mice.** Mice were injected with a dose of 10 mg/kg.
712 Data in the graph represent the average \pm S.E.M., N = 2-3.
713

714 **Fig. 5. Prediction of the interaction between AC1 and ST034307.** (a) Cartoon
715 representation of the AC1 model, showing its catalytic domain (C1a, in red, and
716 C2a, in green) complexed to $G\alpha_s$ (in blue), ST034307 (in cyan or purple), ATP (in
717 yellow), and two magnesium ions (Mg^{2+} , in green). Predicted poses of ST034307,
718 using Gold (b) and Autodock Vina (c) programs, presenting hydrogen-bond
719 (interrupted purple line) and steric interactions. The AC1 residue structures are
720 shown as ball and stick models, the ST034307 inhibitor and ATP as stick models,
721 and Mg^{2+} ions as sphere models using UCSF Chimera program.⁴⁷ All the structures
722 are colored by atom: the nitrogen atoms are shown in blue, the oxygen atoms in
723 red, the chlorine atoms in green, the hydrogen atoms in white, and the carbon chain
724 in gray, cyan, or purple. Non-polar hydrogens have been omitted for clarity.
725
726
727
728
729
730
731
732
733
734
735
736
737
738
739
740
741
742
743
744
745
746
747
748
749
750
751
752
753

754

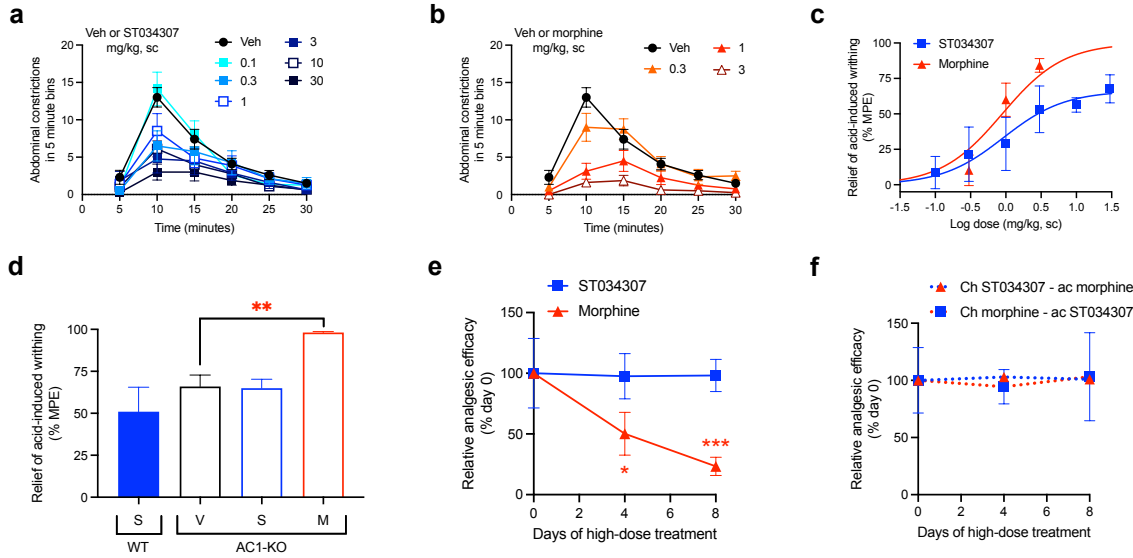
Figure 1



755
756
757
758
759
760
761
762
763
764
765
766
767
768
769
770
771

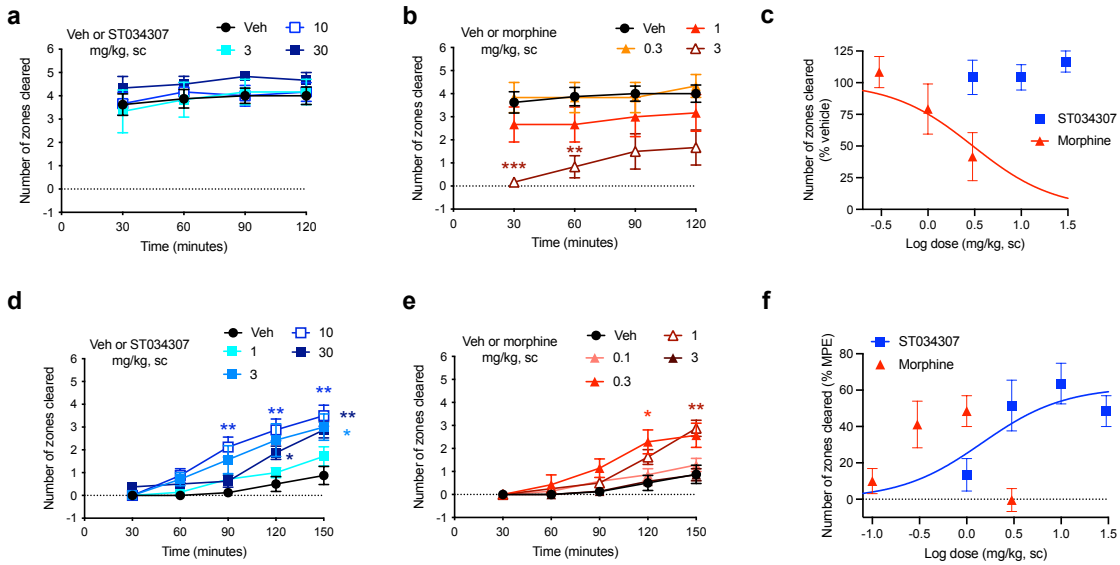
772
773

Figure 2



774
775
776
777
778
779
780
781
782
783
784
785
786

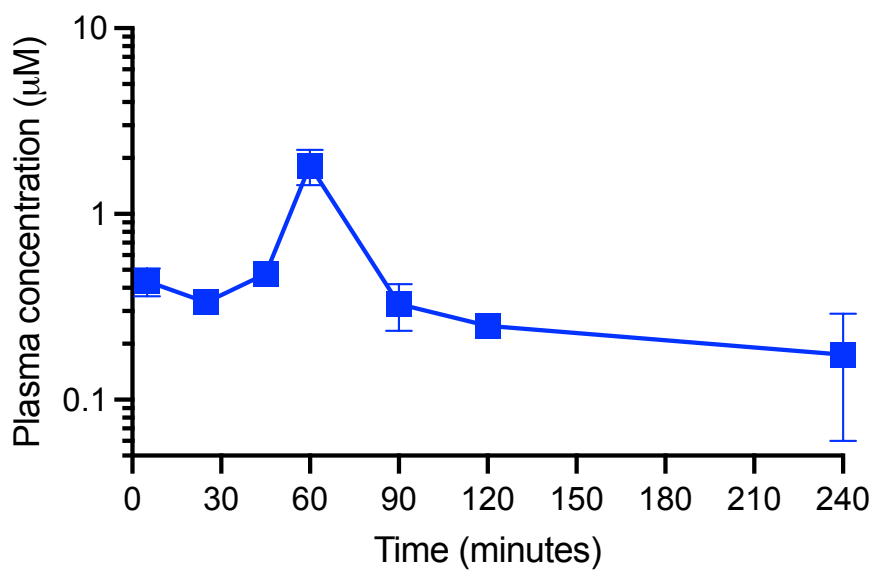
Figure 3



787
788
789
790
791
792

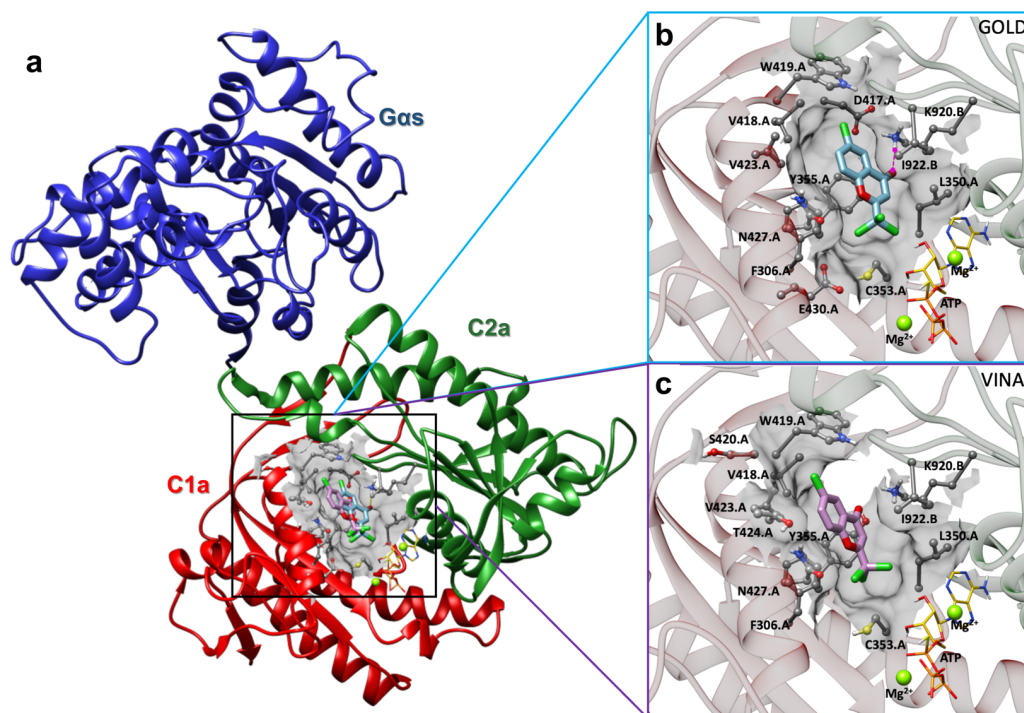
793
794

Figure 4



795
796
797
798
799
300
301
302
303

Figure 5



304